

# From Geometry to Topology: Inverse Theorems for Distributed Persistence

Elchanan Solomon

Department of Mathematics,  
Duke University  
Durham, USA  
yitzchak.solomon@duke.edu

Alexander Wagner

Department of Mathematics,  
Duke University  
Durham, USA  
alexander.wagner@duke.edu

Paul Bendich

Department of Mathematics, Duke University  
Geometric Data Analytics  
Durham, USA  
paul.bendich@duke.edu

**Abstract**—What is the “right” topological invariant of a large point cloud  $X$ ? Prior research has focused on estimating the full persistence diagram of  $X$ , a quantity that is very expensive to compute, unstable to outliers, and far from a sufficient statistic. We therefore propose that the correct invariant is not the persistence diagram of  $X$ , but rather the collection of persistence diagrams of many small subsets. This invariant, which we call “distributed persistence,” is trivially parallelizable, more stable to outliers, and has a rich inverse theory. The map from the space of point clouds (with the quasi-isometry metric) to the space of distributed persistence invariants (with the Hausdorff-Bottleneck distance) is a global quasi-isometry. This is a much stronger property than simply being injective, as it implies that the inverse of a small neighborhood is a small neighborhood, and is to our knowledge the only result of its kind in the TDA literature. Moreover, the quasi-isometry bounds depend on the size of the subsets taken, so that as the size of these subsets goes from small to large, the invariant interpolates between a purely geometric one and a topological one. Lastly, we note that our inverse results do not actually require considering all subsets of a fixed size (an enormous collection), but a relatively small collection satisfying certain covering properties that arise with high probability when randomly sampling subsets. These theoretical results are complemented by two synthetic experiments demonstrating the use of distributed persistence in practice.

## I. INTRODUCTION

Morphometric techniques in data analysis can be loosely divided into the geometric and the topological. Geometric techniques, like landmarks, the Procrustes distance, the Gromov-Hausdorff metric, optimal transport methods, PCA, MDS [Kru64], LLE [RS00], and Isomap [TSL00], are designed to capture some combination of global and local metric structure. Many geometric methods can be solved exactly or approximately via spectral methods, and hence are fast to implement using iterative and sketching algorithms. In contrast, topological techniques, like t-SNE [vdMH08], UMAP [MHM18], Mapper [SMC07], and persistent homology, aim to capture large-scale connectivity structure in data. The growing popularity of t-SNE and UMAP as dimensionality reduction

The first and third authors were partially supported by the Air Force Office of Scientific Research under the grant “Geometry and Topology for Data Analysis and Fusion”, AFOSR FA9550-18-1-0266. The second author was partially supported by the National Science Foundation under the grant “HDR TRIPDS: Innovations in Data Science: Integrating Stochastic Modeling, Data Representations, and Algorithms”, NSF CCF-1934964.

methods suggests that many data sets are topologically, but not metrically, low-dimensional.

The goal of this paper is to introduce a new technique into topological data analysis (TDA) that:

- 1) Provably interpolates between topological and geometric structure (Theorem V.15).
- 2) Is trivially parallelizable.
- 3) Is exactly computable via deterministic and stochastic methods (Porisms V.17 and V.18 and Propositions V.23 and V.25).
- 4) Is provably stable to perturbation of the data (Proposition V.2).
- 5) Is provably invertible, with globally stable inverse (Theorems V.9, V.15, V.21, and Porism V.19).
- 6) Suggests new methods for a host of morphometric challenges, ranging from dimensionality reduction to feature extraction (Section VI).

The theoretical guarantees provided here are, to our knowledge, unmatched by any other method in topological data analysis. The same applies for many spectral methods, which are famously unstable in the presence of a small spectral gap. In addition to these theoretical contributions, we demonstrate our theoretical results empirically on synthetic data sets.

## II. THE DISTRIBUTED TOPOLOGY PROBLEM

Let  $\lambda$  be a statistic of finite point clouds in  $\mathbb{R}^d$ . Let  $X$  be an abstract indexing set with an embedding  $\psi : X \rightarrow \mathbb{R}^d$ . For  $k \in \mathbb{Z}$ , we can define a distributed statistic  $\lambda_k$  that maps the *labeled point cloud*  $(X, \psi)$  to the set  $\{(S, \lambda(\psi(S))) \mid S \subset X, |S| = k\}$  if  $k > 0$  and to  $\emptyset$  otherwise. Put another way,  $\lambda_k(X, \psi)$  records the values of  $\lambda$  on subsets of  $\psi(X)$  of a fixed size, together with abstract labels identifying which invariant corresponds to which subset.<sup>1</sup> For the remainder of this paper, we will omit mentioning the embedding  $\psi$ , and will refer to  $X$  as a point cloud, unless it becomes important to disambiguate between  $X$  as an abstract set and  $X$  as a set with a fixed embedding.

When the computational complexity of  $\lambda$  scales poorly in the size of  $X$ , the statistic  $\lambda_k$  can be easier to compute.

<sup>1</sup>It is also possible to do away with these labels, and we will consider this possibility later on in the paper.

Moreover,  $\lambda_k$  may contain information not accessible via  $\lambda$  itself. We will say that  $\lambda$  is  $k$ -distributed if  $\lambda_k(X)$  determines  $\lambda(X)$  for any subset  $X \subset \mathbb{R}^d$  with  $|X| \geq k$ . Many common geometric invariants are  $k$ -distributed:

- Let  $\lambda$  send a finite set  $X$  to its Euclidean distance matrix. This invariant is  $k$ -distributed for all  $k \geq 2$ .
- Let  $\lambda$  send a finite set  $X$  to its diameter. This invariant is  $k$ -distributed for all  $k \geq 2$ .
- Let  $\lambda$  send a finite set  $X$  to its mean. This invariant is  $k$ -distributed for all  $k \geq 1$ .

The primary theoretical goal of this paper is to address the following three questions:

**Problem II.1.** *Which invariants in applied algebraic topology are  $k$ -distributed for various  $k$ ?*

**Problem II.2.** *If  $\lambda$  is  $k$ -distributed, how much additional topological or geometric information does  $\lambda_k$  contain, as compared to  $\lambda$ , and how does this depend on  $k$ ?*

**Problem II.3.** *Can  $\lambda_k$  be well-approximated, with high probability, using only a small fraction of the total number of subsets of size  $k$ ?*

#### A. Case Study: The Noisy Circle

To illustrate the advantage of working with distributed invariants, we compare three data sets of 500 points. The first is spaced regularly around a circle, the second sampled uniformly from the unit disc, and the third contains 450 points on the circle and 50 points sampled from the disc (we call this the *noisy circle*), see Figure II.1. For each of these point clouds, we compute their full 1-dimensional persistence diagrams, see Figure II.2. In addition, for each point cloud, we sample 1000 subsets of size 10, compute the resulting 1000 1-dimensional persistence diagrams, vectorize them as *persistence images*<sup>2</sup>, and average the results, see Figure II.3. The persistence diagram of the noisy circle is most similar to that of the disc (in Bottleneck distance), demonstrating that ordinary persistence does not see the circle around which most of the data points are clustered. The distributed persistence, however, tells a different story. The distribution for the noisy circle interpolates between the distributions of the other two spaces, but is substantially closer to that of the circle than the disc.

### III. PRIOR WORK ON DISTRIBUTED TOPOLOGY

In [CFL<sup>+</sup>1507], Chazal et al. propose the following framework. Given a metric measure space  $(\mathbb{X}, \rho, \mu)$ , sample  $m$  points and compute the persistence landscape of the associated Vietoris-Rips filtration. This procedure produces a random persistence landscape,  $\lambda$ , whose distribution is denoted  $\Psi_\mu^m$ . Repeating this procedure  $n$  times and averaging produces the empirical average landscape, an unbiased estimator of the average landscape  $E_{\Psi_\mu^m}[\lambda]$ . This approach is similar to

<sup>2</sup>This is a technique for turning a persistence diagram into a function by placing a Gaussian kernel at each dot in the persistence diagram, with mean and variance varying by location, cf. [AEK<sup>+</sup>17].

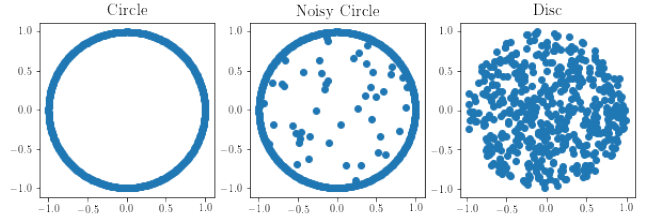


Fig. II.1: Three point clouds: the circle, the noisy circle, and the disc.

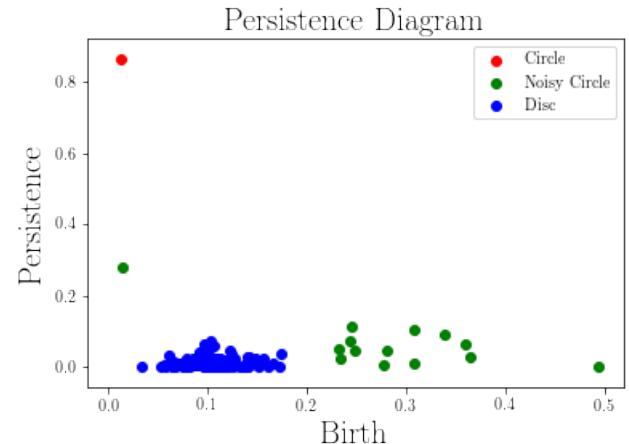


Fig. II.2: The persistence diagrams of our three point clouds, plotted in birth-persistence coordinates.

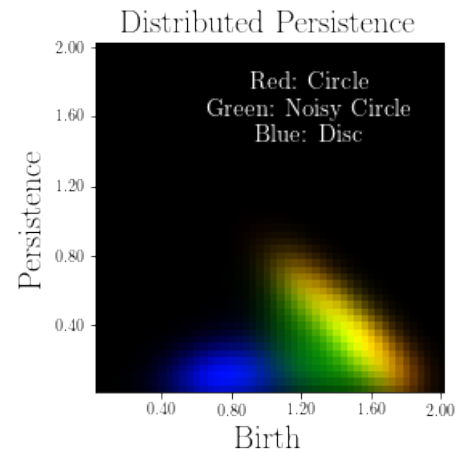


Fig. II.3: Averaged distributed persistence images of our three spaces. The dominant orange/yellow region is the overlay of the circle (red) distribution and the noisy circle (green) distribution.

the distributed topological statistics considered in this paper, except we consider a collection of topological statistics as a labeled set rather than taking their sum. Though Bubenik [Bub20] gives conditions in Theorem 5.11 under which a collection of persistence diagrams may be reconstructed from the average of their corresponding persistence landscapes, such

an inverse exists only generically, and is highly unstable.

The main theorem of [CFL<sup>+</sup>1507] is that the average landscape is stable with respect to the underlying measure. Specifically, if  $\mu$  and  $\nu$  are two probability measures on the same metric space  $(\mathbb{X}, \rho)$ , then the sup norm between induced average landscapes is bounded by  $m^{1/p}W_{\rho, p}(\mu, \nu)$  for any  $p \geq 1$ . Similar results were obtained in [BGMP14] for distributions of persistence diagrams of subsamples. In particular, Blumberg et al. showed that the distribution of barcodes with the Prohorov metric is stable with respect to the associated compact metric measure space with the Gromov-Prohorov metric. Both these results are analogous to the stability of the distributed topological statistics given in Proposition V.2. However, working with labeled collections of distributed topological statistics, we are also able to provide inverse stability results, such as our main Theorem V.15, which states that changes in the metric structure are bounded with respect to changes in the distributed topological statistics.

In [BHPW20], Bubenik et al. consider unit disks, denoted  $D_K$ , of surfaces of constant curvature  $K$  with  $K \in [-2, 2]$ . Since these spaces are all contractible, their reduced singular homology is trivial and global homology cannot distinguish them. However, the authors prove that the maximum Čech persistence for three points sampled from  $D_K$  determines  $K$ . The authors also successfully apply the same empirical framework of average persistence landscapes from [CFL<sup>+</sup>1507] to experimentally determine the curvature of  $D_K$  for various  $K$ . The authors in [DGP<sup>+</sup>16] used average persistence landscapes to provide experimental verification of a known phase transition. Finally, the authors in [MGSH<sup>+</sup>20] use average persistence landscapes to achieve improved results, compared to standard machine learning algorithms, in disease phenotype prediction based on subject gene expressions.

#### IV. BACKGROUND

The content of this paper assumes familiarity with the concepts and tools of persistent homology. Interested readers can consult the articles of Carlsson [Car09] and Ghrist [Ghr08] and the textbooks of Edelsbrunner and Harer [EH10] and Oudot [Oud15]. We include the following primer for readers interested in a high-level, non-technical summary.

Persistent homology records the way topology evolves in a parametrized sequence of spaces. To apply persistent homology to a point cloud, a pre-processing step is needed that converts the point cloud into such a sequence. The two classical ways of doing this are called the Rips and Čech filtrations, respectively; the former is much easier to compute than the latter, at the expense of some geometric fidelity. Both consist of inserting simplices into the point cloud at a parameter value equal to the proximity of the associated vertex points. As the sequence of spaces evolves, the addition of certain edges or higher-dimensional simplices changes the homological type of the space – these simplices are called critical. Persistent homology records the parameter values at which critical simplices appear, notes the dimension in which the homology changes, and pairs critical values by matching

the critical value at which a new homological feature appears to the critical value at which it disappears. This information is organized into a data structure called a persistence diagram, and there are a number of metrics with which persistence diagrams can be compared.

If one forgets about the pairing and retains only the dimension information of the critical values, the resulting invariant is called a Betti curve. Betti curves are simpler to compute and work with than persistence diagrams, but are less informative and harder to compare. Finally, if one also drops the dimension information by taking the alternating sum of the Betti curves, one gets an Euler curve. Euler curves are even less discriminative than Betti curves, but enjoy the special symmetry properties of the Euler characteristic. These symmetries will be put to good use in this paper.

Persistence theory guarantees that a small modification to the parametrization of a sequence of spaces implies only small changes in its persistence diagram. To be precise, if the appearance time of any given simplex is not delayed or advanced by more than  $\epsilon$ , the persistence diagram as a whole is not distorted by more than  $\epsilon$  in the appropriate metric (called the *Bottleneck distance*). Throughout this paper we will use the trick of modifying filtrations by rounding their critical values to a fixed, discrete set.

As a rule, the map sending a point cloud to its persistence diagram is not injective, as many different point clouds share the same persistence diagram. Moreover, the set of point clouds sharing a common persistence diagram need not be bounded, so that arbitrarily distinct point clouds might have the same persistence. There are a number of constructions in the TDA literature that attempt to correct this lack of injectivity by constructing more sophisticated invariants; these are often called *topological transforms*. Examples include the Persistent Homology Transform [TMB14] and Intrinsic Persistent Homology Transform [OS17]; consult [OS20] for a survey of inverse results in persistence. These methods are largely unfeasible to compute exactly, unstable, and provide no global Lipschitz bounds on their inverse, so two wildly different spaces may produce arbitrarily similar (though not exactly identical) transforms. The distributed topology invariant studied in this paper is injective, practically computable, stable, and with Lipschitz inverse.

#### V. THEORETICAL RESULTS

In what follows, we let  $\lambda$  be any of the following four topological invariants:

- Rips Persistence (RP).
- Rips Euler Curve (RE).
- Čech Persistence (CP).
- Čech Euler Curve (CE).

To be precise, RP and CP consist of persistence diagrams for every homological degree. When working with either of these invariants, the Bottleneck or Wasserstein distance is the maximum of the Bottleneck or Wasserstein distances over all degrees.

### A. Stability

A result of the following form is standard in the TDA literature, and demonstrates the ease of producing stable invariants using persistent homology.

**Definition V.1.** Let  $(X, d_X)$  and  $(Y, d_Y)$  be metric spaces. A map  $\phi : (X, d_X) \rightarrow (Y, d_Y)$  is an  $\epsilon$ -quasi-isometry if  $|d_X(x_1, x_2) - d_Y(\phi(x_1), \phi(x_2))| \leq \epsilon$  for all  $x_1, x_2 \in X$ .

**Proposition V.2.** Let  $\phi : (X, d_X) \rightarrow (Y, d_Y)$  be an  $\epsilon$ -quasi-isometry of metric spaces. Then for all subsets  $S \subseteq X$ , and  $\lambda$  either RP or CP,  $d_B(\lambda(S), \lambda(\phi(S))) \leq \epsilon$ , where  $d_B$  is the Bottleneck distance on persistence diagrams.

*Proof.* This follows immediately from the Gromov-Hausdorff stability theorem for persistence diagrams of point clouds [CDSGO16, CSEH07].  $\square$

### B. $k$ -Distributivity

In this section, we show how many distributed invariants suffice to determine the isometry type of a point cloud. This provides an answer to Problem II.1. To help motivate this result, we consider the simple cases of  $k = 2$  and  $k = 3$ .

**Lemma V.3.** All of our  $\lambda$  are 2-distributed. Moreover, the knowledge of  $\lambda_2$  determines the isometry type of  $X$ .

*Proof.* Regardless of the invariant used, it is possible to read off the distances between any pair of points in  $X$ . This determines the embedding of  $X$  up to rigid isometry (see [Sin08]), and hence the Rips and Čech filtrations.  $\square$

Setting  $k = 3$  is sufficient to break the implication of an isometry.

**Lemma V.4.**  $\lambda_3$  does not determine the isometry type of  $X$ .

*Proof.* A simple counterexample suffices. Let  $X$  consist of the vertices of an obtuse triangle with angle  $\theta > \pi/2$ . Varying the angle  $\theta$  in  $(\pi/2, \pi)$  alters the isometry type of  $X$ , but leaves its topology unchanged.  $\square$

To obtain stronger results, we introduce the following two generalizations, one to the notion of distributivity, and the other to the invariants  $\lambda$ .

**Definition V.5.** We say that  $\lambda$  is  $(k_1, k_2, \dots, k_r)$ -distributed if  $\lambda_{k_1}$  through  $\lambda_{k_r}$ , taken together, determine  $\lambda$ .

**Definition V.6.** For any of our four invariants  $\lambda$ , let  $\lambda^m$  be the modified invariant restricted to the  $m$ -skeleton of the Rips or Čech complex. In other words, they are persistence invariants of filtrations whose top simplices have dimension  $m$ .

Setting  $m = 0$  provides information only on the cardinality of  $X$ . The 1-skeleton contains both geometric and topological information, and its persistence is fast to compute. As  $m$  increases, computational complexity goes up, and the resulting invariants record higher-dimensional topological information. The following lemma demonstrates how knowing sufficiently many Euler characteristic invariants allows one to determine new ones.

**Lemma V.7.** Let  $\lambda$  be RE or CE. For any point cloud  $X$  and  $k \geq m + 2$ ,  $\{\lambda_k^m, \lambda_{k-1}^m, \dots, \lambda_{k-m-1}^m\}$  determine  $\lambda_2^m$ .

*Proof.* Let  $Y \subset X$  be a subset of size  $(k - m - 2)$ . Let  $\{x_1, \dots, x_{m+2}\}$  be points in  $X \setminus Y$ , set  $W = Y \cup \{x_1, \dots, x_{m+2}\}$  and  $Y_i = W \setminus \{x_i\}$ . Then  $|W| = k$  and  $|Y_i| = (k - 1)$  for all  $i$ . Note that every subset of size  $(m + 1)$  in  $W$  is contained in some  $Y_i$ . Thus if we write  $K^m(W)$  to denote the  $m$ -skeleton of the full simplex on  $W$ , we have  $K^m(W) = \bigcup_i K^m(Y_i)$ , and the same equality holds true when the full simplex is replaced with the Rips or Čech complex at a fixed scale  $r$ . Note that in general,  $K^m(S) \cap K^m(T) = K^m(S \cap T)$  for any subsets  $S, T \subset X$ , but the same equality does not hold with intersections replaced with unions, as there may be simplices in  $K^m(S \cup T)$  whose set of vertices are not contained in either  $S$  or  $T$ . This explains why we take all  $Y_1, \dots, Y_{m+2}$  to cover  $W$ .

Let us now apply the inclusion-exclusion property of the Euler characteristic to compare the Euler characteristic of  $W$  (at a given scale  $r$ ) with those of the  $Y_i$ .

$$\begin{aligned} \chi(W^r) &= \chi\left(\bigcup_i Y_i^r\right) \\ &= \sum_i \chi(Y_i^r) \\ &\quad - \sum_{i < j} \chi(Y_i^r \cap Y_j^r) \\ &\quad + \sum_{i < j < k} \chi(Y_i^r \cap Y_j^r \cap Y_k^r) \\ &\quad \dots \\ &\quad + (-1)^{m+3} \chi(Y_1^r \cap \dots \cap Y_{m+2}^r) \end{aligned}$$

The resulting alternating sum involves all pairwise intersections of the  $Y_i$ , and only a single union term,  $\lambda^m(W)$ . By hypothesis, we know the Euler characteristics of all pairwise intersections of cardinality at least  $k - m - 1$ . The only unknown term in the sum is  $\lambda^m(Y)$ , which we can then solve for, completing the proof. See Figure V.1 for an concrete example.  $\square$

**Corollary V.8.** Let  $\lambda$  be RE or CE. For any point cloud  $X$  and  $k \geq m + 2$ ,  $\{\lambda_k^m, \lambda_{k-1}^m, \dots, \lambda_{k-m-1}^m\}$  determine  $\lambda_2^m$ .

*Proof.* Lemma V.7 shows that  $\{\lambda_k^m, \lambda_{k-1}^m, \dots, \lambda_{k-m-1}^m\}$  determines  $\lambda_{k-m-2}^m$ . By the same logic,  $\{\lambda_{k-1}^m, \lambda_{k-2}^m, \dots, \lambda_{k-m-2}^m\}$  determines  $\lambda_{k-m-3}^m$ . Repeating this argument, we can deduce  $\lambda_2^m$ .  $\square$

Leveraging Lemma V.7, we prove that all of our persistence invariants are appropriately distributed.

**Theorem V.9.** For any of the four invariants  $\lambda$ , the  $m$ -skeleton invariant  $\lambda^m$  is  $(k, k-1, \dots, k-m-1)$ -distributed for all  $k \geq m+1 \geq 2$ . Moreover,  $\{\lambda_k^m, \lambda_{k-1}^m, \dots, \lambda_{k-m-1}^m\}$  determine the isometry type of  $X$ .

*Proof.* When  $m \geq 1$ , the  $m$ -skeleton contains all edges in  $X$ , so Lemma V.3 still applies. If the set  $\{k, k-1, k-$

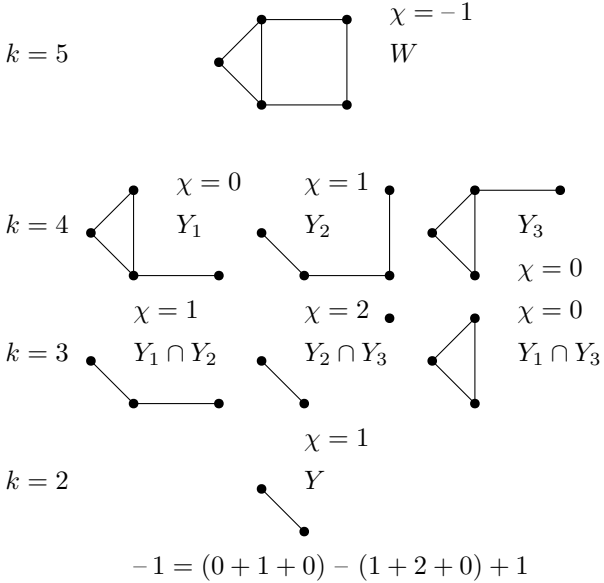


Fig. V.1: Our goal is to deduce the Euler Characteristic (at a fixed scale  $r$ ) of  $Y$ , a 1-simplex consisting of  $k = 2$  points. This can be derived from the Euler Characteristics of the other subcomplexes in the diagram above.

$2, \dots, k - m - 1\}$  contains 2, this follows from Lemma V.3. Otherwise, let us assume  $\lambda$  is either RE or CE, as RP or CP contain strictly more information than their Euler characteristic counterparts. By Corollary V.8, we can determine  $\lambda_2^m$  and then apply Lemma V.3.  $\square$

**Remark V.10.** Note that  $m = 1$  is sufficient to apply the prior theorem. As  $m$  gets larger, more topological information is needed to determine the isometry type of the underlying space.

### C. Approximate Distributivity

We now consider what happens if two point clouds have distributed invariants which are similar but not identical. We show that this implies a quasi-isometry between  $X$  and  $Y$ , with constant depending quadratically on the subset size parameter  $k$ . This provides a precise answer to Problem II.2 on how the distributed statistic interpolates between geometry and topology.

The key insight in the proof of this result is that there is always a way to modify the Rips or Čech filtrations on  $X$  and  $Y$  to force their distributed invariants to coincide exactly. Taken together with the telescoping trick of Corollary V.8, this modified invariant must agree for all subsets of size two. Persistence stability allows us to assert that the modified invariant and the original persistence invariant are a bounded distance apart, so equality of the modified invariant gives near-equality of the Rips or Čech persistences on subsets of size two, which is nothing more than pairwise distance data.

The proposed modification to our filtration consists of rounding it to a discrete set of values. The following technical lemma shows how to pick a rounding set  $R$  that aligns two

sets of points without moving any point more than a bounded amount.

**Lemma V.11** (Rounding Lemma). *Let  $P = \{p_1 \leq p_2 \leq \dots \leq p_N\}$  and  $Q = \{q_1, q_2, \dots, q_N\}$  be two sets of real numbers. Define  $d_i = |p_i - q_i|$ , let  $\epsilon = \max d_i$  and  $\delta = \sum_{i=1}^n d_i$ . Then there exists a subset  $R \subset \mathbb{R}$  and a map  $\pi : P \cup Q \rightarrow R$  sending a point  $x$  to the unique closest element in  $R$  (rounding up at midpoints), with:*

- 1)  $\pi(p_i) = \pi(q_i)$  for all  $i$ .
- 2)  $|\pi(x) - x| \leq 3\epsilon + 4\delta$ .

In particular, since  $\epsilon \leq \delta$ , we can replace (2) with (2\*)  $|\pi(x) - x| \leq 7\delta$ .

*Proof.* The proof is a recursive construction. The first step is to add  $p_1$  to  $R$ . We then repeat the following argument, iterating through  $P$ . Consider  $p_n$ , and let  $r_*$  be the largest element of  $R$  so far. If  $p_n < r_* + 2\epsilon + 4\delta$ , skip  $p_n$ . Otherwise, initialize  $r_n = p_n$ , and iterate over all  $i < n$  and check that  $p_i > (r_n + r_*)/2$  iff  $q_i > (r_n + r_*)/2$ . Every time an index  $i$  is found for which this condition is violated, increment  $r_n \leftarrow r_n + 2d_i$ . The effect of this incrementation is to force both  $q_i$  and  $p_i$  to be strictly closer to  $r_*$  than they are to  $r_n$ . This condition can be violated at most once for each  $p_i$ , hence the total sum of the incrementation is  $2\delta$ , at the end of which  $r_n$  is added to  $R$ .

Let us see why the resulting set  $R$  satisfies (1) and (2). If  $r_n$  was added to  $R$ , then it is at most  $2\delta$  from  $p_n$  and  $2\delta + \epsilon$  from  $q_n$ , whereas  $|r_* - p_n| > 2\epsilon + 4\delta$  and  $|r_* - q_n| > \epsilon + 4\delta$  by the triangle inequality. Thus  $\pi(q_n) = \pi(p_n) = r_n$ . For  $i < n$ , the recursive incrementation ensures  $\pi(p_i) = r_n$  if and only if  $\pi(q_i) = r_n$ , and otherwise the value of  $\pi$  on  $(p_i, q_i)$  is unchanged. Thus (1) is preserved. To check (2), note that if  $\pi(p_i) = \pi(q_i) = r_n$  for  $i < n$ , then  $p_i$  and  $q_i$  are closer to  $r_n$  than any other element in  $R$ . By recursive hypothesis, this distance is at most  $3\epsilon + 4\delta$ , so  $|p_i - r_n|$  and  $|q_i - r_n| \leq 3\epsilon + 4\delta$ .

If, on the other hand, no point was added to  $R$ , then  $p_n < r_* + 2\epsilon + 4\delta$ . Let  $p_* \in P$  be the point corresponding to  $r_*$ . Since  $r_* + 2\epsilon + 4\delta > p_n \geq p_* \geq r_* - 2\delta$ , we know  $|p_n - r_*| \leq 2\epsilon + 4\delta$  and  $|q_n - r_*| \leq |q_n - p_n| + |p_n - r_*| \leq 3\epsilon + 4\delta$ . If we can show that  $\pi(p_n) = r_*$  and  $\pi(q_n) = r_*$ , the proof will be complete. If  $p_n \geq r_*$  then it is clear that  $\pi(p_n) = r_*$ , and similarly, if  $q_n \geq r_*$ , we have  $\pi(q_n) = r_*$ . Thus we need to consider what happens if  $p_n$  or  $q_n$  are strictly less than  $r_*$ .

Let  $r_{**} < r_*$  be the penultimate point in  $R$ . Our goal is to show that  $p_n$  or  $q_n$  are strictly closer to  $r_*$  than they are to  $r_{**}$ . Recall the point  $p_* \in P$  corresponding to  $r_*$ . Since  $p_* \leq p_n$  and  $|r_* - p_*| \leq 2\delta$ , we know that  $p_n \geq r_* - 2\delta$  and  $q_n \geq r_* - 2\delta - \epsilon$ . Thus if  $p_n$  or  $q_n$  are strictly less than  $r_*$ , they are no further than  $2\delta$  and  $2\delta + \epsilon$  away, respectively. However, since  $|r_* - r_{**}| \geq 2\epsilon + 4\delta$ , the triangle inequality implies that  $|p_n - r_{**}| \geq 2\epsilon + 2\delta$  and  $|q_n - r_{**}| \geq \epsilon + 2\delta$ .

Thus, if  $p_n$  or  $q_n$  are smaller than  $r_*$ , they must still round up  $r_*$  than  $r_{**}$ , and not  $r_{**}$  or any other element of  $R$ .  $\square$

**Corollary V.12.** *We can extend the set  $R$  in the Rounding Lemma to a  $14\delta$ -dense subset  $R' \subset \mathbb{R}$ , without changing  $\pi$  on  $P \cup Q$ . All that is necessary is to enrich  $R$  by adding points in  $(\cup_{r \in R} N(r, 14\delta))^C$ .*

With our rounding trick in hand, we can now prove the central result of this section, Theorem V.15. The following pieces of notation clarify the statement and proof of the theorem:

**Definition V.13.** Let  $m < k$  be natural numbers. We define the following partial sum of binomial coefficients:

$$S(k, m) = \binom{k}{2} + \binom{k}{3} + \cdots + \binom{k}{m+1}$$

**Definition V.14.** Let  $(K, f)$  be a filtered simplicial complex, i.e. a simplicial complex  $K$  with a real-valued function  $f : K \rightarrow \mathbb{R}$  encoding the appearance times of simplices. Given a subset  $R \subset \mathbb{R}$ , rounding this filtration to  $R$  consists of post-composing  $f$  with the map sending every element of  $\mathbb{R}$  to its nearest element in  $R$  (rounding up at midpoints). Thus, the simplices in the rounding filtration appear only at values contained in  $R$ . The effect of rounding on the resulting persistence diagrams is to round the birth and death times of its constituent dots; no new points are introduced.

**Theorem V.15.** *Let  $\lambda$  be either RP or CP, and take  $k > m > 0$ . Let  $\phi : X \rightarrow Y$  be a bijection such that for all  $S \subseteq X$  with  $|S| \in \{k, k-1, \dots, k-m-1\}$ ,  $d_B(\lambda^m(S), \lambda^m(\phi(S))) \leq \epsilon$ . If  $\lambda$  is RP,  $\phi$  is a  $112k^2\epsilon$  quasi-isometry, and if  $\lambda$  is CP,  $\phi$  is a  $224S(k, m)k^{m+1}\epsilon$  quasi-isometry.*

*Proof.* Let  $(x_1, x_2)$  be an edge in  $X$ , and let  $(y_1, y_2)$  be the corresponding edge in  $Y$ . Let  $S \subseteq X$  be a subset of size  $k$  containing  $(x_1, x_2)$ . Let  $A(S)$  be the set of appearance times of simplices in the  $m$ -skeleton of  $S$ , and define  $A(\phi(S))$  similarly. Apply the Rounding Lemma to the following set of pairs:

$$\{(l, l+2\epsilon), (l, l-2\epsilon) \mid l \in A(S) \cup A(\phi(S))\}$$

In the language of the hypotheses of the Rounding Lemma, we have  $\delta = \sum d_i = 4\epsilon|S(A)| + 4\epsilon|S(\phi(A))|$ . Let  $R$  be the subset given by the Rounding Lemma and its corollary, and let  $\lambda^R$  denote the invariant  $\lambda^m$  with filtration rounded to  $R$ . Note that if  $S' \subset S$  has the property that  $d_B(\lambda^m(S'), \lambda^m(\phi(S'))) \leq \epsilon$ , then  $\lambda^R(S') = \lambda^R(\phi(S'))$ . To see why this is the case, let  $p = (a, b) \in \lambda^R(S') \cup \Delta$  and  $p' = (a', b') \in \lambda^R(\phi(S')) \cup \Delta$  be dots paired in an optimal Bottleneck matching, where  $\Delta$  is the diagonal.

Let us first assume that  $p$  is on the diagonal, so that  $|b' - a'| \leq 2\epsilon$ . If  $p'$  is also on the diagonal, then both  $p$  and  $p'$  remain on the diagonal after rounding to  $R$  (or, indeed, rounding to any set of values). If  $p'$  is not on the diagonal,  $a', b' \in A(\phi(S))$ ; since  $|b' - a'| \leq 2\epsilon$ ,  $a'$  and  $b'$  are rounded to the same point in  $R$ , and hence the point  $(a', b')$  is rounded to the diagonal.

If  $p$  is not on the diagonal, then  $a, b \in A(S)$ , and since  $a' \in [a - \epsilon, a + \epsilon]$  and  $b' \in [b - \epsilon, b + \epsilon]$ , we can conclude that  $a$  and  $a'$  round to the same point in  $R$ , and the same is true for  $b$  and  $b'$ . In any case, the points  $p$  and  $p'$  become identical after rounding to  $R$ . Thus, using  $\lambda^R$ ,  $\phi$  preserves persistence diagrams of all subsets of  $S$  of size  $k$  through  $k-m-1$ , and hence, by Corollary V.8, all subsets of size two, in particular  $(x_1, x_2)$ . Thus,  $\lambda^R((x_1, x_2)) = \lambda^R((y_1, y_2))$ <sup>3</sup>. As  $R$  is  $(4 \times 14)\epsilon|S(A)| + (4 \times 14)\epsilon|S(\phi(A))|$  dense in  $\mathbb{R}$ , persistence stability implies that  $\lambda^m$  and  $\lambda^R$  are within  $56\epsilon(|S(A)| + |S(\phi(A))|)$  of each other in Bottleneck distance. The triangle inequality then tells us that  $d_B(\lambda^m(x_1, x_2), \lambda^m((y_1, y_2))) \leq 112\epsilon(|S(A)| + |S(\phi(A))|)$ , which is equivalent to  $\|x_1 - x_2\| - \|y_1 - y_2\| \leq 112\epsilon(|S(A)| + |S(\phi(A))|)$ . To conclude the proof, note that for the Rips complex,  $|S(A)|, |S(\phi(A))| \leq \binom{k}{2} = \frac{k^2 - k}{2} \leq \frac{k^2}{2}$ , as all appearance times of simplices are just pairwise distances between points. For the Čech complex, there may be a total of  $S(k, m)$  distinct appearance times in  $S(A)$  or  $S(\phi(A))$ , one for each simplex of dimension between 1 and  $m$ , that need to be rounded correctly (all dimension zero simplices necessarily appear at height zero).  $\square$

**Remark V.16.** Theorem V.15 answers Problem II.2 by showing that smaller values of  $k$  give more control of quasi-isometry type than larger values. This justifies our claim that distributed topology interpolates between local geometry and global topology.

Moving on to Problem II.3, the following two porisms, resulting from the proof of Theorem V.15, show that our inverse results do not require checking *all* subsets with cardinality  $k$  through  $k-m-1$ , but a much smaller collection that covers the space  $X$  in the right way. Subsection V-E bounds the number of randomly selected subsets needed to produce such a covering with high probability.

**Porism V.17.** *The results of Theorem V.15 do not require  $\phi$  to preserve the topology for all subsets  $S$  with  $|S| \in \{k, k-1, \dots, k-m-1\}$ . Rather, it suffices to consider a collection  $C$  of subsets of  $X$  with the following properties:*

- (Covering property) *For every subset  $\sigma$  of  $X$  with  $|\sigma| \leq 2$ , there is a subset  $S \in C$  containing  $\sigma$  with  $|S| = k$ .*
- (Closure property) *If  $S \in C$  has  $|S| = k$ , and  $S' \subset S$  has  $|S'| \geq k-m-1$ , then  $S' \in C$ .*

*This requires checking many fewer subsets of  $X$ , rather than  $\binom{|X|}{k} + \binom{|X|}{k-1} + \cdots + \binom{|X|}{k-m-1}$ .*

One can often check even fewer subsets by replacing the covering property with a  $\delta$ -dense version:

- ( $\delta$ -dense covering property) *There exists a subset  $X' \subseteq X$  with  $|X'| \geq k$ , such that  $X'$  is  $\delta$ -dense in  $X$  and  $\phi(X')$  is  $\delta$ -dense in  $Y$ , and such that for every subset  $\sigma$  of  $X'$  with  $|\sigma| = 2$ , there is a subset  $S \in C$  containing  $\sigma$  with  $|S| = k$ .*

<sup>3</sup>Noting that for subsets of size two, Euler curves and persistence diagrams contain identical information.

The resulting bound is not in the quasi-isometry distance but in the Gromov-Hausdorff distance.

**Porism V.18.** *Let  $\lambda$  be either RP or CP, and take  $k > m > 0$ . Let  $\phi : X \rightarrow Y$  be a bijection between metric spaces, and let  $C$  be a collection of subsets of cardinality between  $k$  and  $k-m-1$  that satisfies both the  $\delta$ -dense covering property and the closure property. Suppose that  $d_B(\lambda^m(S), \lambda^m(\phi(S))) \leq \epsilon$  for all  $S \in C$ . If  $\lambda$  is RP, then  $d_{GH}(X, Y) \leq 112k^2\epsilon + 2\delta$ , and if  $\lambda$  is CP, then  $d_{GH}(X, Y) \leq 224S(k, m)k^{m+1}\epsilon + 2\delta$ .*

*Proof.* The proof of Theorem V.15 implies that  $\phi$  is a quasi-isometry from  $X'$  to  $\phi(X')$ . We can extend this to a a Gromov-Hausdorff matching between  $X$  and  $Y$ , and two applications of the triangle inequality increase the bound by  $2\delta$ .  $\square$

**Porism V.19.** *If  $X \subset \mathbb{R}^{d_1}$  and  $Y \subset \mathbb{R}^{d_2}$ , then the quasi-isometry bound for Čech persistence in the prior theorem can be replaced with:*

$$112k^2 \left( \epsilon + \sqrt{\frac{2d_1}{d_1+1}} + \sqrt{\frac{2d_2}{d_2+1}} \right)$$

*Note that the added terms sum at most to  $2\sqrt{2}$ , so that this bound is better than the bound given in Porism V.18 for non-infinitesimal  $\epsilon$ , but does fail to go to 0 as  $\epsilon \rightarrow 0$ .*

*Proof.* The Rips and Čech persistence of point clouds in  $\mathbb{R}$  are always within  $\sqrt{\frac{2d}{d+1}}$  of one another in the bottleneck distance, cf. Theorem 2.5 in [DSG07]. The result then follows by replacing Čech persistence with Rips persistence and using the triangle inequality.  $\square$

#### D. Topology + Sparse Geometry

Our goal now is improve the results of the prior section by giving quasi-isometry bounds that scale linearly in  $k$ , rather than quadratically. This can be accomplished by using an inclusion-exclusion argument on the 1-skeleton persistence of  $X$  that uses only subsets of size  $k$  and  $(k-1)$ . Namely, given a subset  $Y \subset X$  with  $|Y| = (k-2)$ , we take  $Y = Y_1 \cap Y_2$  for  $|Y_1| = |Y_2| = (k-1)$  and  $W = (Y_1 \cup Y_2)$  with  $|W| = k$ , as shown in Figure V.2, and attempt to deduce the Euler characteristic of  $Y$  from those of  $Y_1$ ,  $Y_2$ , and  $W$ . However, the union of the 1-skeleton complexes on  $Y_1$  and  $Y_2$  is not the 1-skeleton complex on  $W$ , owing to the fact that  $W$  contains an extra edge connecting the pair of vertices in  $W \setminus Y$ .

The effect of this extra edge on persistence is quite subtle, but its effect on the Euler curve is trivial, as it amounts to subtracting a step function supported on  $[r, \infty)$ , where  $r$  is the appearance time of the extra edge in the complex. If we knew  $r$ , we could correct the deficit in our inclusion-exclusion argument. Note that the we have the freedom to choose  $Y_1$  and  $Y_2$  as we like, so to make this argument work we need only know the length of a single edge in  $X$  that does not intersect  $Y$ . A very small collection of edge lengths suffice to patch up the inclusion-exclusion argument for all subsets of  $X$  of size at most  $k$ . Before proving our quasi-isometry bound, we need the following corollary of the Rounding Lemma.

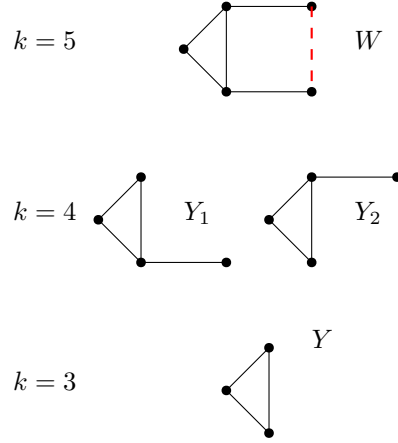


Fig. V.2: Our goal is to deduce the Euler Characteristic (at a fixed scale  $r$ ) of  $Y$ , a subcomplex of size  $k = 3$ , using subcomplexes of size  $k = 4$  and  $k = 5$ . However, the inclusion-exclusion argument fails because the union of the complexes of  $Y_1$  and  $Y_2$  is not the complex on  $W = Y_1 \cup Y_2$ , and the missing edge is shown in red.

**Lemma V.20.** *Given  $A_1 \cdots A_n$  and  $B_1 \cdots B_n$  persistence diagrams, with  $W^1(A_i, B_i) \leq \delta$ , there exists a  $28n\delta$ -dense subset  $R \subset \mathbb{R}$  such that rounding all the persistence diagrams to the grid  $R \times R$  forces  $\pi(A_i) = \pi(B_i)$  for all  $i$ .*

*Proof.* This is a straightforward application of the Rounding Lemma. We take the set  $P$  to consist of all the birth and death times of all the dots in the  $A_i$ , and construct  $Q$  from the  $B_i$  similarly. As each  $(A_i, B_i)$  pair contributes two sets of points, births and deaths, the total  $\ell^1$  norm of pairing  $P$  with  $Q$  is  $2 \times n\delta = 2n\delta$ . By Corollary V.12, one can find a subset  $R$  of density  $28n\delta$  which ensures  $\pi(p_i) = \pi(q_i)$  for all matched pairs  $p_i \in P, q_i \in Q$ , and hence  $\pi(A_i) = \pi(B_i)$  for all  $i$ .  $\square$

**Theorem V.21.** *Let  $\lambda$  be either RP or CP, and take  $k > m = 1$ . Let  $\phi : X \rightarrow Y$  be a bijection such that for all  $S \subseteq X$  with  $|S| \in \{k, k-1\}$ ,  $W^1(\lambda^1(S), \lambda^1(\phi(S))) \leq \epsilon_1$ . Suppose further that there is a subset  $X' \subset X$  of size  $(k-1)$  with*

$$\sum_{(x_i, x_j) \in X' \times X'} \|\|x_i - x_j\| - \|\phi(x_i) - \phi(x_j)\|\| \leq \epsilon_2.$$

*Then  $\phi$  is a  $56(k+1)\epsilon_1 + 28\epsilon_2$  quasi-isometry.*

*Proof.* Let  $x_1, x_2$  be a pair of points in  $X$ . Without loss of generality, we can assume that at least one of these points is not in  $X'$ , as the proof is otherwise trivial. Thus, we can extend  $x_1, x_2$  to a subset  $S$  of size  $k$  by adding points in  $X'$ .  $S$  has  $k$  subsets of size  $(k-1)$ . The prior lemma tells us that we can find a  $28(k+1)\epsilon_1$ -dense subset  $R \subset \mathbb{R}$  such that  $\lambda^R(S) = \lambda^R(\phi(S))$ , and  $\lambda^R(S') = \lambda^R(\phi(S'))$  for any subset  $S' \subset S$  with  $|S'| = (k-1)$ . We can further demand from the Rounding Lemma that the appearance time of every edge in  $X'$  and every edge in  $\phi(X')$  be exactly the same, where  $R$  will now be  $28(k+1)\epsilon_1 + 14\epsilon_2$  dense in  $\mathbb{R}$ .

Now, for any subset  $S' \subset S$  containing  $(x_1, x_2)$  with size  $|S'| = k - 2$ , the set  $S \setminus S'$  consists of a pair of points  $(p_1, p_2) \in X'$ . We then know that  $\lambda^R(S') = \lambda^R(\phi(S'))$  by using an inclusion-exclusion calculation with  $S' \cup p_1, S' \cup p_2$ , and  $S' \cup p_1 \cup p_2$ , since the missing term in the inclusion-exclusion formula is exactly the same for both  $X$  and  $Y$ , after rounding to  $R$ . This argument can be iterated on the entire sublattice of  $S$  consisting of those subsets  $S' \subset S$  with  $|S'| \leq k - 2$  and which contain  $(x_1, x_2)$ . The proof concludes by an identical stability analysis to that of Theorem V.15.  $\square$

**Remark V.22.** The above proof does not require all pairwise distances in  $X'$ , as the inclusion-exclusion trick can be carried out with  $O(k)$  intersections, rather than the full sublattice of  $O(k^2)$  intersections. We have omitted this analysis as it obfuscates the statement of the theorem and does not significantly improve it.

#### E. Probabilistic Results

Propositions V.17 and V.18 tell us that we do not need to sample all  $\binom{|X|}{k} + \binom{|X|}{k-1} + \cdots + \binom{|X|}{k-m-1}$  subsets  $S \subseteq X$  of size  $|S| \in \{k, \dots, k-m-1\}$ , so long as the collection  $C$  of subsets considered satisfies appropriate cover and closure properties. The goal of this section is to give bounds on the probability that a randomly chosen collection of subsets of size  $k$  has the covering property. The closure property can then be ensured by adding subsets of the appropriate cardinalities.

**Proposition V.23.** Let  $X$  be a set of size  $n$ , and choose  $M$  subsets  $\{S_1, \dots, S_M\}$  of size  $k$  by uniform sampling without replacement. Let  $p \leq k$  and  $A$  be the outcome that every set of  $p$  points  $(x_1, \dots, x_p)$  is contained in at least one  $S_i$ . Then

$$P(A) \geq 1 - \binom{n}{p} \left(1 - \left(\frac{k-p+1}{n-p+1}\right)^p\right)^M.$$

*Proof.*

$$P(A) = 1 - P(\exists (x_1, \dots, x_p) \text{ not in any } S_i) \quad (1)$$

$$\geq 1 - \sum_{(x_1, \dots, x_p)} P((x_1, \dots, x_p) \text{ not in any } S_i) \quad (2)$$

$$= 1 - \binom{n}{p} P((x_1, \dots, x_p) \text{ not in any } S_i) \quad (3)$$

$$= 1 - \binom{n}{p} \prod_{i=1}^M P((x_1, \dots, x_p) \text{ not in } S_i) \quad (4)$$

$$= 1 - \binom{n}{p} \prod_{i=1}^M (1 - P((x_1, \dots, x_p) \subseteq S_i)) \quad (5)$$

An elementary counting argument provides:

$$P((x_1, \dots, x_p) \subseteq S_i) = \frac{\binom{n-p}{k-p}}{\binom{n}{k}}$$

Note further that:

$$\frac{\binom{n-p}{k-p}}{\binom{n}{k}} = \frac{k(k-1)(k-2)\cdots(k-p+1)}{n(n-1)(n-2)\cdots(n-p+1)} \geq \left(\frac{k-p+1}{n-p+1}\right)^p$$

Finally, observe that the effect of replacing  $P((x_1, \dots, x_p) \subseteq S_i)$  with  $\left(\frac{k-p+1}{n-p+1}\right)^p$  is to decrease the value of (5), and so the result is proved.  $\square$

**Proposition V.24.** Let  $A$  be as in the prior proposition. For any  $\epsilon \in (0, 1)$ , if

$$M \geq (p \log \left(\frac{ne}{p}\right) - \log(1-\epsilon)) \left(\frac{n-p+1}{k-p+1}\right)^p$$

then  $P(A) \geq \epsilon$ .

*Proof.* Our goal is to have:

$$\epsilon \geq 1 - \binom{n}{p} \left(1 - \left(\frac{k-p+1}{n-p+1}\right)^p\right)^M$$

which is equivalent to

$$\binom{n}{p} \left(1 - \left(\frac{k-p+1}{n-p+1}\right)^p\right)^M \geq 1 - \epsilon$$

Taking the log of both sides gives

$$\log \binom{n}{p} + M \log \left(1 - \left(\frac{k-p+1}{n-p+1}\right)^p\right) \geq \log(1-\epsilon)$$

Solving for  $M$  gives:

$$M \geq \frac{\log(1-\epsilon) - \log \binom{n}{p}}{\log \left(1 - \left(\frac{k-p+1}{n-p+1}\right)^p\right)} \quad (6)$$

The denominator on the right-hand side of (6) is negative, so using the identity  $\binom{n}{p} < \left(\frac{ne}{p}\right)^p$ , we can replace (6) with the strictly stronger inequality:

$$M \geq \frac{\log(1-\epsilon) - p \log \frac{ne}{p}}{\log \left(1 - \left(\frac{k-p+1}{n-p+1}\right)^p\right)} \quad (7)$$

We can then apply the identity  $0 \geq -x \geq \log(1-x)$  for  $x \in (0, 1)$ , and so replace (7) with the stronger inequality,

$$M \geq \frac{\log(1-\epsilon) - p \log \frac{ne}{p}}{-\left(\frac{k-p+1}{n-p+1}\right)^p} \quad (8)$$

The result then follows via simple algebra.  $\square$

The following proposition can be used to bound the probability that a collection  $C$  is a  $\delta$ -dense covering.

**Proposition V.25.** Suppose that the set  $X$  has a probability measure  $\mu$  and can be covered by  $s$  subsets  $\{X_1, \dots, X_s\}$  with measure  $\mu(X_i) \geq 1/s$ . Choose  $\{S_1, \dots, S_M\}$  subsets of size  $k$  according to  $\mu$ . Let  $A$  be the outcome that for every collection of  $p$  subsets  $\{X_{i_1}, \dots, X_{i_p}\}$ , there exists some  $S_i$  such that  $S_i \cap X_{i_j} \neq \emptyset$  for all  $j$ . Then

$$P(A) \geq 1 - \binom{s}{p} \left(1 - \left(\frac{k-p+1}{s-p+1}\right)^p\right)^M$$

*Proof.* Construct the set  $\tilde{X}$  whose points are the sets  $\{[X_1], \dots, [X_s]\}$ . A subset  $S \subseteq X$  maps to subset  $\tilde{S} \subseteq \tilde{X}$

in the following way:  $\tilde{S}$  contains  $[X_i]$  if  $S \cap X_i \neq \emptyset$ . It is evident that the outcome  $A$  is equivalent to the condition that any  $\{[X_{i_1}], \dots, [X_{i_p}]\}$  is contained in some  $\tilde{S}_i$ . Let  $B$  be the same outcome, with a different sampling procedure: instead of randomly picking subsets  $S \subset X$  and constructing  $\tilde{S}$ , pick subsets  $\tilde{S}$  uniformly in  $\tilde{X}$  directly. It is clear that  $P(A) \geq P(B)$ , because  $\mu(X_i) \geq 1/s$  means that the likelihood of  $\tilde{S}$  containing  $[X_i]$  is higher for the first sampling procedure than the second. But Proposition V.23 implies that

$$P(B) \geq 1 - \binom{s}{p} \left(1 - \left(\frac{k-p+1}{s-p+1}\right)^p\right)^M$$

□

Let us explain how to produce such a measure  $\mu$ . Given  $\phi : X \rightarrow Y$ , we define  $d_\phi(x_1, x_2) = \max\{\|x_1 - x_2\|, \|\phi(x_1) - \phi(x_2)\|\}$ . Using furthest point sampling, we can produce a subset  $\{x_1, \dots, x_s\}$  of  $X$  that is  $\delta$ -dense in  $d_\phi$  for some  $\delta$ , and let  $X_i = N(x_i, \delta)$ . We define  $\mu$  on  $X$  via the following mixed sampling procedure: we randomly pick a subset  $X_i$  and then uniformly sample its elements. The resulting measure  $\mu$  satisfies the hypotheses of the prior proposition, and a  $\delta$ -dense covering  $C$  can be obtained with high probability by sampling i.i.d. from  $\mu$ .

## VI. APPLICATIONS

Let us return to viewing  $X$  as an abstract set, and  $\psi : X \rightarrow \mathbb{R}^d$  an embedding that turns  $X$  into a point cloud. The distributed topology  $\lambda_k$  of  $X$ , as we defined it, is  $\{(S, \lambda(\psi(S))) \mid S \subset X, |S| = k\}$ . It is often also necessary to consider the un-labeled invariant  $\{\lambda(\psi(S)) \mid S \subset X, |S| = k\}$ , particularly in situations when distributed persistence is a feature extraction method. As we list some applications of distributed persistence below, we will take care to identify if the invariant needed is labeled or unlabeled.

- (Dimensionality Reduction) When the target dimension of  $\psi : X \rightarrow \mathbb{R}^d$  is too high, we may wish to learn a lower-dimensional embedding  $\pi : X \rightarrow \mathbb{R}^{d'}$ . We can force  $\pi$  to preserve the topological structure of  $\psi$  by minimizing the following sum over  $\{S \subset X \mid |S| = k\}$ :

$$\sum_S d_B(\lambda(\psi(S)), \lambda(\pi(S)))$$

This application uses labeled distributed topology.

- (Shape Registration) Given two embedded point clouds  $X$  and  $Y$  modeling the same shape, it can be of interest to learn a map  $f : X \rightarrow Y$  aligning corresponding points. This can be accomplished by having  $f$  minimize the following sum over  $\{S \subset X \mid |S| = k\}$ :

$$\sum_S d_B(\lambda(S), \lambda(f(S)))$$

This application uses labeled distributed topology.

- (Feature Extraction) Given an embedded point cloud  $X$ , we can consider the unlabeled set  $\{\lambda(\psi(S)) \mid S \subset X, |S| = k\}$  as a bag-of-features invariant. These features

can be vectorized, averaged, transformed into a measure, and in any other way summarized, before being fed into a standard supervised or unsupervised machine learning pipeline.

## VII. EXPERIMENTS

Suppose  $X$  and  $Y$  are finite subsets of Euclidean spaces and  $\phi : X \rightarrow Y$  is a bijection between them. Theorem V.15 shows that we may test if  $\phi$  is a quasi-isometry by evaluating  $d_B(\lambda^m(S), \lambda^m(\phi(S)))$  for a certain collection of subsets  $S \subseteq X$ . If  $X$  is fixed and  $Y$  is variable, we can minimize  $d_B(\lambda^m(S), \lambda^m(\phi(S)))$  thanks to the differentiability of persistence computations; this has the effect of bringing  $Y$  closer in alignment with  $X$ . Moreover, Porisms V.17 and V.18 and the probabilistic results in Section V-E show that correcting a relatively small number of subsets  $S \subseteq X$  is likely to force a quasi-isometry.

In the following two synthetic experiments, we follow the methodology described above for  $X$  as (1) 100 points evenly distributed on a circle in  $\mathbb{R}^2$  and (2) 256 points evenly distributed on a torus in  $\mathbb{R}^3$ . The codomain  $Y$  is initialized to be  $X$  with independent Gaussian noise added coordinate-wise. Our aim is to see whether minimizing a distributed topological functional via gradient descent succeeds in correcting for the large geometric distortion of adding Gaussian noise. In both cases, every iteration step consists of uniformly sampling  $k = 25$  points, denoted  $S$ , from  $X$  and taking a step (i.e. perturbing  $Y$ ) to minimize the loss  $W_2^2(D_0(S), D_0(\phi(S))) + W_2^2(D_1(S), D_1(\phi(S)))$ , where  $D_i$  is the degree  $i$  persistence diagram of the Rips filtration. Because we are updating  $Y$  based on only a single sample  $S$ , we use the Adam optimizer [KB14] to benefit from momentum. The first (resp. second) row in Figure VII.1 show the initial state of  $Y$ ,  $Y$  after  $1e5$  (resp.  $1e6$ ) iterations, and  $Y$  after  $2e5$  (resp.  $2e6$ ) iterations. For both experiments, we observe the codomain space  $Y$  re-organizing itself to closely resemble  $X$ . The coloring of the points in Figure VII.1 denotes their labeling in  $X$ , so that nearby points have similar colors. The fact that the color gradients in the final positions of  $Y$  are largely continuous affirm that our optimization fixes not only the global geometry of  $Y$ , but also the labeled pairwise distances, and hence gives a space quasi-isometric to  $X$ .

## VIII. CONCLUSION

It has long been understood that computational complexity and sensitivity to outliers are major challenges in the application of persistent homology in data analysis. Moreover, the lack of a stable inverse makes it very hard to say which geometric information is retained in a persistence diagram, and which is forgotten. Multiple lines of research have sought to address these problems by constructing more sophisticated topological invariants and tools, such as the persistent homology transform, multiparameter persistence, distributed persistence calculations [ZXG<sup>+</sup>19] and discrete Morse theory. However, any gains in invertibility are compromised by sizeable increases in computational complexity.

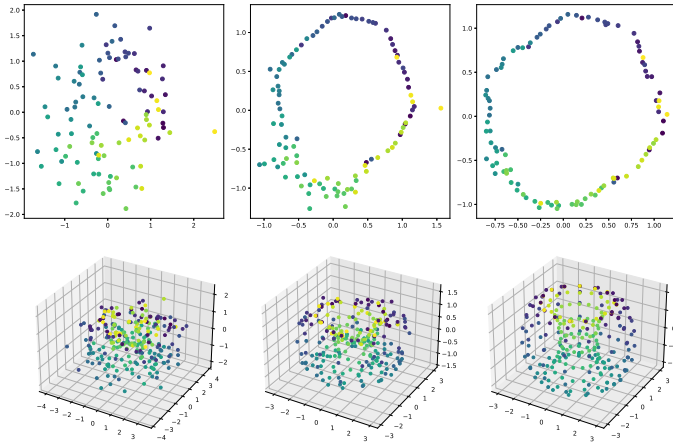


Fig. VII.1: Synthetic optimization experiments. Columns correspond to initial, intermediate, and final positions of  $Y$ . Color denotes labelling.

The focus of this paper was the simplest scheme for speeding up persistence calculations: subsampling. Subsampling and bootstrapping are ubiquitous in machine learning and are already being applied in topological data analysis. What we have shown is that this simple approach also enjoys uniquely strong theoretical guarantees. In particular, the manner in which distributed persistence interpolates between geometry and topology is explicitly given by quadratic bounds. Moreover, these theoretical guarantees are complemented by the success that subsampling has seen in the TDA literature, and the robust synthetic experiments shown above.

There remain a number of outstanding problems, both theoretical and computational, that would complement the results of this paper and facilitate its practical application.

- Distributed persistence, as we have defined it, depends on an alignment of two data sets. In practice, we use it as an unlabeled bag of features. What injectivity results can be obtained in this unstructured setting?
- Individual persistence diagrams can be challenging to work with, due to the fact that the space of diagrams admits no Hilbert space structure [CB19, BW20, Wag19], though there are a number of effective vectorizations in the literature. How can these be extended or adapted to provide vectorizations of sets of persistence diagrams coming from subsamples of a fixed point cloud? This is a more structured problem than working with arbitrary collections of persistence diagrams.
- If we are interested in recovering the global topology of  $X$  rather than its quasi-isometry or Gromov-Hausdorff type, it suffices to estimate pairwise distances between points in adjacent Voronoi cells, at least when working with the full Rips or Čech complex and not a skeleton. A careful analysis of this setting could dramatically decrease the Lipschitz constants appearing in Theorem V.15.

## REFERENCES

[AEK<sup>+</sup>17] Henry Adams, Tegan Emerson, Michael Kirby, Rachel Neville, Chris Peterson, Patrick Shipman, Sofya Chepushtanova, Eric Hanson, Francis Motta, and Lori Ziegelmeier, *Persistence images: A stable vector representation of persistent homology*, The Journal of Machine Learning Research **18** (2017), no. 1, 218–252. ↑2

[BGMP14] Andrew J. Blumberg, Itamar Gal, Michael A. Mandell, and Matthew Pancia, *Robust statistics, hypothesis testing, and confidence intervals for persistent homology on metric measure spaces*, Foundations of Computational Mathematics **14** (2014), no. 4, 745–789. ↑3

[BHPW20] Peter Bubenik, Michael Hull, Dhruv Patel, and Benjamin Whittle, *Persistent homology detects curvature*, Inverse Problems **36** (2020jan), no. 2, 025008. ↑3

[Bub20] Peter Bubenik, *The persistence landscape and some of its properties*, Topological data analysis, 2020, pp. 97–117. ↑2

[BW20] Peter Bubenik and Alexander Wagner, *Embeddings of persistence diagrams into hilbert spaces*, Journal of Applied and Computational Topology **4** (2020), no. 3, 339–351. ↑10

[Car09] Gunnar Carlsson, *Topology and data*, Bulletin of the American Mathematical Society **46** (2009), no. 2, 255–308. ↑3

[CB19] Mathieu Carrière and Ulrich Bauer, *On the metric distortion of embedding persistence diagrams into separable Hilbert spaces*, 35th International Symposium on Computational Geometry, 2019, pp. Art. No. 21, 15. MR3968607 ↑10

[CDSGO16] Frédéric Chazal, Vin De Silva, Marc Glisse, and Steve Oudot, *The structure and stability of persistence modules*, Springer, 2016. ↑4

[CFL<sup>+</sup>1507] Frédéric Chazal, Brittany Fasy, Fabrizio Lecci, Bertrand Michel, Alessandro Rinaldo, and Larry Wasserman, *Subsampling methods for persistent homology*, Proceedings of the 32nd international conference on machine learning, 201507, pp. 2143–2151. ↑2, 3

[CSEH07] David Cohen-Steiner, Herbert Edelsbrunner, and John Harer, *Stability of persistence diagrams*, Discrete & computational geometry **37** (2007), no. 1, 103–120. ↑4

[DGP<sup>+</sup>16] Irene Donato, Matteo Gori, Marco Pettini, Giovanni Petri, Sarah De Nigris, Roberto Franzosi, and Francesco Vaccarino, *Persistent homology analysis of phase transitions*, Phys. Rev. E **93** (2016May), 052138. ↑3

[DSG07] Vin De Silva and Robert Ghrist, *Coverage in sensor networks via persistent homology*, Algebraic & Geometric Topology **7** (2007), no. 1, 339–358. ↑7

[EH10] Herbert Edelsbrunner and John Harer, *Computational topology: an introduction* (2010). ↑3

[Ghr08] Robert Ghrist, *Barcodes: the persistent topology of data*, Bulletin of the American Mathematical Society **45** (2008), no. 1, 61–75. ↑3

[KB14] Diederik P Kingma and Jimmy Ba, *Adam: A method for stochastic optimization*, arXiv preprint arXiv:1412.6980 (2014). ↑9

[Kru64] J. B. Kruskal, *Multidimensional scaling by optimizing goodness of fit to a nonmetric hypothesis*, Psychometrika **29** (1964), no. 1, 1–27. ↑1

[MGSH<sup>+</sup>20] Sayan Mandal, Aldo Guzmán-Sáenz, Niina Haiminen, Saugata Basu, and Laxmi Parida, *A topological data analysis approach on predicting phenotypes from gene expression data*, Algorithms for computational biology, 2020, pp. 178–187. ↑3

[MHM18] Leland McInnes, John Healy, and James Melville, *Umap: Uniform manifold approximation and projection for dimension reduction*, arXiv preprint arXiv:1802.03426 (2018). ↑1

[OS17] Steve Oudot and Elchanan Solomon, *Barcode embeddings for metric graphs*, arXiv preprint arXiv:1712.03630 (2017). ↑3

[OS20] Steve Oudot and Elchanan Solomon, *Inverse problems in topological persistence*, Topological data analysis, 2020, pp. 405–433. ↑3

[Oud15] Steve Y Oudot, *Persistence theory: from quiver representations to data analysis*, Vol. 209, American Mathematical Society Providence, 2015. ↑3

[RS00] Sam T. Roweis and Lawrence K. Saul, *Nonlinear dimensionality reduction by locally linear embedding*, Science **290** (2000),

no. 5500, 2323–2326, available at <https://science.sciencemag.org/content/290/5500/2323.full.pdf>. ↑1

[Sin08] Amit Singer, *A remark on global positioning from local distances*, Proceedings of the National Academy of Sciences **105** (2008), no. 28, 9507–9511. ↑4

[SMC07] Gurjeet Singh, Facundo Memoli, and Gunnar Carlsson, *Topological Methods for the Analysis of High Dimensional Data Sets and 3D Object Recognition*, Eurographics symposium on point-based graphics, 2007. ↑1

[TMB14] Katharine Turner, Sayan Mukherjee, and Doug M Boyer, *Persistent homology transform for modeling shapes and surfaces*, Information and Inference: A Journal of the IMA **3** (2014), no. 4, 310–344. ↑3

[TSL00] Joshua B. Tenenbaum, Vin de Silva, and John C. Langford, *A global geometric framework for nonlinear dimensionality reduction*, Science **290** (2000), no. 5500, 2319–2323, available at <https://science.sciencemag.org/content/290/5500/2319.full.pdf>. ↑1

[vdMH08] Laurens van der Maaten and Geoffrey Hinton, *Visualizing data using t-sne*, Journal of Machine Learning Research **9** (2008), no. 86, 2579–2605. ↑1

[Wag19] Alexander Wagner, *Nonembeddability of Persistence Diagrams with  $p > 2$  Wasserstein Metric*, arXiv e-prints (October 2019), arXiv:1910.13935, available at 1910.13935. ↑10

[ZXG<sup>+</sup>19] Simon Zhang, Mengbai Xiao, Chengxin Guo, Liang Geng, Hao Wang, and Xiaodong Zhang, *Hypha: A framework based on separation of parallelisms to accelerate persistent homology matrix reduction*, Proceedings of the ACM international conference on supercomputing, 2019, pp. 69–81. ↑9